Journal of Organometallic Chemistry 694 (2009) 3306–3311

Contents lists available at ScienceDirect

Journal of Organometallic Chemistry

journal homepage: www.elsevier.com/locate/jorganchem

Two-dimensional supramolecular networks generated from weak Ag···C_{py} interactions: Synthesis, structural, thermal and fluorescence studies of silver(I) complexes of 5,5-diethylbarbiturato with pyridine-2-ylmethanol and 2,6-dimethoxypyridine

Veysel T. Yilmaz [a,*], Eda Soyer [a], Orhan Buyukgungor [b]

[a] Department of Chemistry, Faculty of Arts and Sciences, Uludag University, 16059 Bursa, Turkey
[b] Department of Physics, Faculty of Arts and Sciences, Ondokuz Mayis University, 55139 Kurupelit, Samsun, Turkey

ARTICLE INFO

Article history:
Received 29 April 2009
Received in revised form 4 June 2009
Accepted 5 June 2009
Available online 9 June 2009

Keywords:
5,5-Diethylbarbiturate
Pyridine-2-ylmethanol
2,6-Dimethoxypyridine
Supramolecular network
Ag···C interaction

ABSTRACT

Two new silver(I) complexes [Ag(barb)(pym)]·H_2O (**1**) and [Ag(barb)(dmpy)]·1.5H_2O (**2**) (barb = 5,5-diethylbarbiturate, pym = pyridine-2-ylmethanol and dmpy = 2,6-dimethoxypyridine) have been synthesized and characterized by elemental analysis, IR spectroscopy and single crystal X-ray diffraction. In both complexes, the silver(I) ions are linearly coordinated by the N atoms of a barb anion and a pym or a dmpy ligand, forming mononuclear species. The molecules of **1** and **2** are doubly bridged by N–H···O hydrogen bonds involving the barb moieties and these hydrogen-bonded dimers are assembled into two-dimensional layered networks through weak Ag···C_{py} (η^1) interactions of *ca.* 3.3 Å. Additionally, the thermal and fluorescent properties of these complexes are also investigated.

1. Introduction

Barbiturates are a group of drugs derived from barbituric acid (malonylurea or 4-hydroxyuracil). They act as depressants of the central nervous system and have powerful sedative and hypnotic properties. The medicinal properties of barbiturates mainly depend on the side groups attached to the pyrimidine ring [1].

Zwikker prepared the first metal complex of 5,5-diethylbarbituric acid (barbH) in pyridine (py), [Cu(barb)$_2$(py)$_2$] [2] and such complexes were used in the detection and identification of these drugs. Copper(II) complexes of different barbiturates with py were prepared by Levi and Hubley [3], while mixed-ligand barb complexes with different metal ions, [M^{II}(barb)$_2$(im)$_2$] (M^{II} = Co and Zn; im = imidazole) [4], [Ni(isoamylbarb)$_2$(im)$_2$] [5], [Cu(barb)$_2$(py)$_2$] [6], [Cu(barb)$_2$(pic)$_2$]·2H_2O [7] and [Zn(barb)$_2$(pic)$_2$] (pic = picoline) [8] appeared in this field. X-ray studies showed that the barb ligand in these complexes coordinates to metals via the deprotonated N atom.

Recently, we synthesized a number of barb complexes and explored different coordination modes of the barb ligand in the case of different metal ions and co-ligands [9–15]. These studies clearly indicate that the barb anion is a polyfunctional ligand due to the presence of several potential donor atoms such as two amine nitrogen and three carbonyl oxygen atoms. In this work, we report the synthesis, structural characterization of two new barb-silver(I) complexes with pyridine-2-ylmethanol (pym) and 2,6-dimethoxypyridine (dmpy), namely [Ag(barb)(pym)]·H_2O (**1**) and [Ag(barb)(dmpy)]·1.5H_2O (**2**). X-ray crystal structures of both complexes have shown that these complexes consist of mononuclear species, which are connected by weak Ag···C_{py} interactions into two-dimensional network. Such an interaction was observed in the silver(I) complexes of barb for the first time and the significance of the Ag···C_{py} interactions are discussed. Moreover, the thermal and photoluminescence properties of these compounds are studied.

2. Experimental

2.1. Materials and measurements

All reagents were purchased and used as supplied. The elemental analyses (C, H and N) were performed on a Costech Elemental Analyser. IR spectra were recorded on a Thermo Nicolet 6700 FT-IR spectrophotometer as KBr pellets in the frequency range 4000–400 cm^{-1}. Thermal analysis curves (TG and DTA) were obtained from a Seiko Exstar TG/DTA 6200 thermal analyzer in a dynamic air atmosphere with a heating rate of 10 K min^{-1} using a

* Corresponding author. Tel.: +90 224 2941749; fax: +90 224 2941 898.
E-mail address: vtyilmaz@uludag.edu.tr (V.T. Yilmaz).

0022-328X/$ - see front matter © 2009 Elsevier B.V. All rights reserved.
doi:10.1016/j.jorganchem.2009.06.006

sample size of 5–10 mg and platinum crucibles. Excitation and emission spectra of the ligands and their solid complexes were recorded at room temperature with a Varian Cary Eclipse spectrophotometer equipped with a Xe pulse lamp of 75 kW, using excitation and emission slits of 20 nm.

2.2. Synthesis of the silver(I) complexes

Na(barb) (5,5-diethylbarbituric acid sodium salt) (0.21 g, 1 mmol) dissolved in water (10 ml) was added to a solution of $AgNO_3$ (0.17 g, 21 mmol) in water (10 ml) with stirring at room temperature. The solution immediately became milky. The addition of pyridine-2-ylmethanol (pym) (0.10 ml) together with a mixture of 2-propanol (PrOH) and acetonitrile (MeCN) (1:1) (10 mL) to the milky suspension resulted in a clear solution. The final solution was allowed to stand in darkness at room temperature and colorless prisms of $[Ag(barb)(pym)]\cdot H_2O$ (**1**) were obtained after 3 days. Yield 77%. M.p. 141 °C (decomp). Anal. Calc. for $C_{14}H_{20}AgN_3O_5$: C, 40.2; H, 4.8; N, 10.1. Found: C, 40.4; H, 4.5; N, 10.3%. IR (cm^{-1}): 3395sb, 3191mb, 3085w, 2974w, 2929vw, 2868w, 1716s, 1675vs, 1638vs, 1601vs, 1458w, 1422vs, 1364vs, 1336sh, 1315vs, 1258s, 1164vw, 1103vw, 1062w, 1005w, 833w, 764s, 698w, 645vw, 613vw, 543m, 474w, 449w.

$[Ag(barb)(dmpy)]\cdot 1.5H_2O$ (**2**) was synthesized in a similar way using dmpy instead of pym. Yield 65%. M.p. 100 °C (decomp). Anal. Calc. for $C_{15}H_{23}AgN_3O_{6.5}$: C, 39.4; H, 5.1; N, 9.2. Found: C, 39.7 H, 5.5; N, 9.4%. IR (cm^{-1}): 3470sb, 3184sb, 3086w, 3028w, 2969w, 2936vw, 2875w, 1712s, 1676vs, 1634vs, 1605vs, 1553s, 1460w, 1423vs, 1369vs, 1319vs, 1257s, 1166vw, 1140vw, 1070w, 1023m, 948w, 844w, 791m, 764m, 730vw, 695w, 542m, 474w, 444w.

2.3. X-ray crystallography

The data collection was performed at 150 K on a Stoe-IPDS-2 diffractometer equipped with a graphite monochromated Mo Kα radiation ($\lambda = 0.71073$ Å). The data reduction and numerical absorption correction were performed using the X-RED program [16]. The structures were solved by direct methods using SHELXS97 [17] and refined on F^2 by a full-matrix least-squares using SHELXL97 [17]. All non-hydrogen atoms were easily found from the difference Fourier map and refined anisotropically. Hydrogen atoms bonded to C and N atoms were refined using a riding model, with C–H = 0.96–0.97 Å and N–H = 0.86–0.91 Å. The constraint $U_{iso}(H) = 1.2U_{eq}$(C and N) or $1.5U_{eq}$(methyl C) was applied. The H atoms of water molecules in **1** were refined freely. The unit cell of **2** has an accessible solvent volume of 92.5 Å^3, which are occupied by severely disordered water molecules. Therefore, the water molecules were eliminated from the refinement of the structure by means of the SQUEEZE subroutine of PLATON and the *hkl* intensities were modified accordingly [18]. Details of crystal data, data collection, structure solution and refinement are given in Table 1.

3. Results and discussion

3.1. Synthesis and IR characterization

The direct reactions between stoichiometric amounts of $AgNO_3$ and Na(barb) were carried out in the presence of pym or dmpy in a PrOH/MeCN solution (1/1) at room temperature and afforded the complexes **1** and **2** in good yields, as colorless crystalline solids, which were fully characterized (see Section 2). Both compounds are stable in solid state and soluble in the warm EtOH/MeCN mixture (1:1).

Selected FTIR spectral data for **1** and **2** are given in Table 2. The strong and broad absorption bands at 3395 cm^{-1} for **1** and 3461 cm^{-1} for **2** are assigned to the ν(OH) vibrations of the lattice water molecules. The ν(NH) stretching of the barb ligands appears as a distinct band at 3191 cm^{-1} and 3184 cm^{-1} for **1** and **2**, respectively. The multiple weak bands in the range 2830–3095 cm^{-1} are attributed to the C–H stretching vibrations. The three sharp bands in the frequency range 1630–1720 cm^{-1} characterize the carbonyl group vibrations of the barb ligands. The barb ligand exists in triketo form and the carbonyl groups do not participate in coordination in these complexes. Compared to that of Na(barb), the apparent red-shifts may, therefore, be associated with strong hydrogen bonding associated with the carbonyl groups. The four of five intense bands between 1605 and 1315 cm^{-1} corresponds to both in-plane vibrations of the C–C bonds, and C–H deformation vibrations, while the C–N stretchings occur as strong bands centered at *ca.* 1258 cm^{-1}.

3.2. Description of the crystal structures

The molecular structures of **1** and **2** are shown in Figs. 1 and 2, respectively. Selected bond lengths and angles are listed in Table 3 together with the hydrogen bond parameters. Complexes **1** and **2**

Table 1
Crystallographic data and structure refinement for **1** and **2**.

	1	**2**
Formula	$C_{14}H_{20}AgN_3O_5$	$C_{15}H_{20}AgN_3O_5$
Molecular weight	418.20	430.21
Temperature (K)	150(2)	150(2)
Wavelength (Å)	0.71073	0.71073
Crystal system	Orthorhombic	Triclinic
Space group	*Pbca*	$P\bar{1}$
Unit cell dimensions		
a (Å)	7.2174(2)	6.8619(3)
b (Å)	13.6482(6)	11.4893(5)
c (Å)	32.9402(10)	12.3456(5)
α (°)	90	100.611(3)
β (°)	90	97.995(4)
γ (°)	90	96.317(4)
Volume (Å^3)	3244.8(2)	938.12(7)
Z	8	2
Calculated density (g/cm^3)	1.712	1.523
μ (mm^{-1})	1.271	1.101
F(0 0 0)	1696	436
Crystal size (mm^3)	0.58 × 0.41 × 0.16	0.55 × 0.35 × 0.07
θ range (°)	2.47–26.74	1.82–26.50
Index ranges (*h*, *k*, *l*)	−8/9; −17/16; −38/41	−8/8; −14/14; −15/15
Reflections collected	13 830	14 445
Independent reflections [$R_{(int)}$]	3425 [0.0328]	3889 [0.0489]
Reflections observed (>2σ)	3006	3662
Absorption correction	Numerical	Numerical
Data/parameters	3425/217	3889/217
Goodness-of-fit (GOF) on F^2	1.054	1.022
Final *R* indices [$I > 2\sigma(I)$]	$R_1 = 0.0260$, $wR_2 = 0.0691$	$R_1 = 0.0246$, $wR_2 = 0.0624$
Largest difference peak and hole (e Å^{-3})	0.443 and −0.838	0.442 and −0.520

Table 2
Selected FTIR spectral data[a] for **1** and **2**.

Assignment	**1**	**2**
ν(OH)	3395sb	3461sb
ν(NH)	3191mb	3184sb
ν(CH)	3085w, 2974w, 2929vw, 2868w	3085w, 2970m, 2929vw, 2868w
ν(CO)	1716s, 1675vs, 1638vs	1715s, 1675vs, 1638vs
ν(CC)	1601vs	1605vs
δ(CH)	1422vs, 1364vs, 1315vs	1423vs, 1369vs, 1319vs
ν(CN)	1258s	1257vs

[a] Frequencies in cm^{-1}. b = broad; m = medium; w = weak; vw = very weak; vs = very strong; s = strong; sh = shoulder.

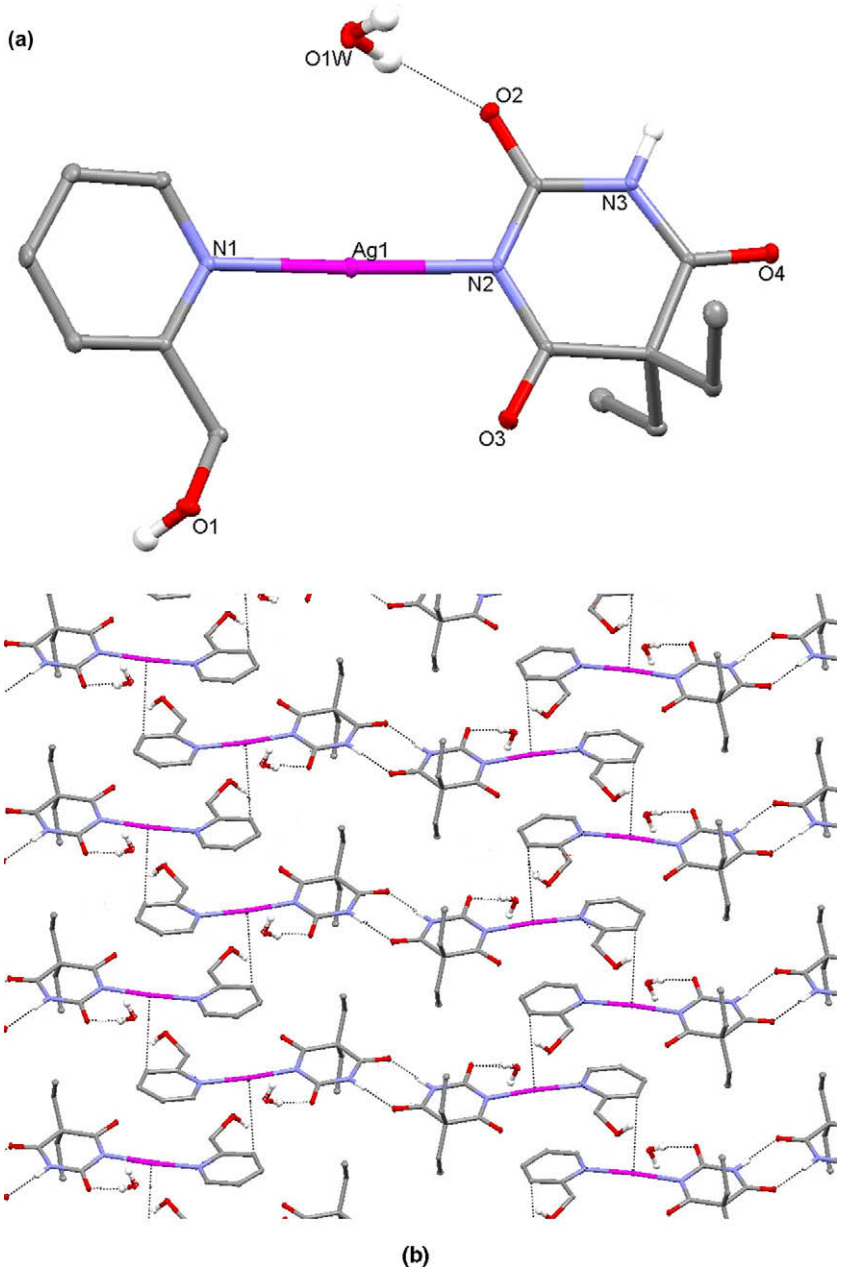

Fig. 1. (a) Molecular structure of [Ag(barb)(pym)]·H_2O (**1**). CH hydrogen atoms are omitted for clarity. (b) A fragment of 2D network of **1**, showing N–H···O and Ag···C interactions viewed down b.

crystallize in the orthorhombic (*P*bca) and triclinic crystal system ($P\bar{1}$), respectively. The silver(I) ion in **1** is coordinated by a neutral pym ligand and a barb anion, while in **2** by the dmpy and barb ligands. The AgN_2 geometry is slightly distorted linear with N–Ag–N angles of 174.61(6)° in **1** and 173.83(6)° in **2**. The Ag–N_{barb} bond distance of **1** is slightly longer than that of **2**. The Ag–N_{barb} bond distances in both complexes are significantly longer than those found in the reported silver(I)-barb complexes, $Na_3[Ag_3(\mu\text{-barb})_6]$ [10], $\{[Ag_2(\mu\text{-barb})_2][Ag_2(\mu\text{-en})_2]\cdot 5H_2O\}_n$ [10], [Ag(barb)(bpy)] [13] and [Ag(barb)(pypr)] [13], but they are somewhat shorter than the corresponding distances found in [Ag(barb)(μ-bpe)]$_n$ [10].

The pyrimidine rings of the barb ligands in **1** and **2** are essentially planar and the three carbonyl groups are not significantly displaced from the mean planes of the rings. The py rings of pym and dmpy ligands are also planar. The OH group of pym is displaced from the mean plane of the py ring by 0.432(3) Å, whereas both methoxy groups of dmpy are in the mean plane of the py ring. The dihedral angles between the py and barb rings are 9.06(2)° in **1**, and 53.44(3)° in **2**. Compared that in **1**, the larger dihedral angle in **2** may be due to the steric hindrance of two OMe groups of the dmpy ligand.

The individual molecules of **1** and **2** are doubly linked into dimers by N–H···O hydrogen bonds involving the barb ligands in the neighbouring molecules. As shown in Figs. 1 and 2, the dimeric units are further connected by Ag···C_{py} (η^1) interactions between silver(I) ions and py rings of the adjacent molecules into two-dimensional layered networks extending along the crystallographic *ac* plane. The Ag···C distances in **1** and **2** are 3.322 and 3.245 Å, respectively, which are noticeably shorter than the sum of van der Waals radii of the Ag(I) ion and the carbon atom (3.42 Å). Complexes **1** and **2** are the first examples displaying weak Ag···$C_{py}(\pi)$ interactions with the py ring. Some Ag-containing polymeric complexes generated from aromatic ligands have been

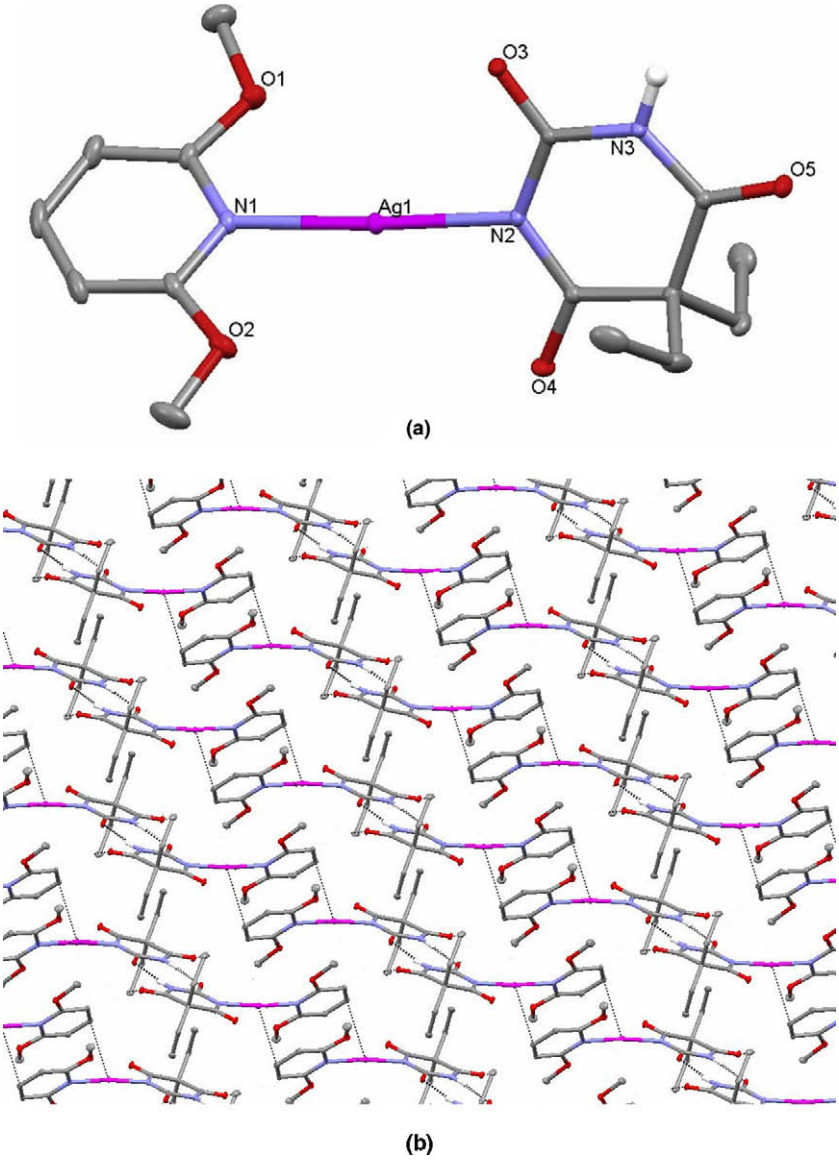

Fig. 2. (a) Molecular structure of [Ag(barb)(dmpy)] (**2**). CH hydrogen atoms are omitted for clarity. (b) A fragment of 2D network of **2**, showing N–H···O and Ag···C interactions viewed down b.

reported to exhibit similar weak Ag···C interactions with Ag···C distances ranging from 2.80 to 3.38 Å [19–26]. Although the Ag···C contacts in **1** and **2** may also be considered as crystal packing effects, it appears that in the present complexes, the weak Ag···C interactions play a highly significant role in the construction of the two-dimensional supramolecular networks and controlling packing of molecules in the solid state.

3.3. Thermal behavior

Thermal decomposition and stability of complexes **1** and **2** were studied by TG and DTA in the temperature range 25–900 °C. The thermal curves of **1** and **2** are illustrated in Fig. 3. Complex **1** is stable up to 80 °C and then, begins to lose its lattice water molecules between 80 °C and 138 °C with a mass loss of 4.5% (calcd. 4.2%). The TG curve shows a continuous mass loss for the decomposition of the anhydrite residue [Ag(barb)(pym)] in the range 140–349 °C and therefore, it is difficult to estimate mass loss of each ligand. However, the two endothermic peaks at 218 and 261 °C corresponds to the elimination of the pym ligand, while a highly exothermic peak centered at 336 °C characterizes the degradation of the barb moiety. The experimental mass loss for this stage is 70.0% which well agrees

Table 3
Selected bond and hydrogen bonding geometry for complexes **1** and **2**.

Bonds lengths (Å) and angles (°)		**1**		**2**
Ag1–N1		2.152(2)		2.136(2)
Ag1–N2		2.120(2)		2.107(2)
N1–Ag1–N2		174.61(6)		173.83(6)
D–H···A	D–H (Å)	H···A (Å)	D···A (Å)	D–H···A (°)
Hydrogen bonds[a]				
1				
O1W–H1W···O2	0.83(2)	1.92(2)	2.738(2)	169(3)
N3–H3A···O4^{i}	0.86	1.99	2.850(2)	178
O1–H1A···O1W^{ii}	0.82	1.88	2.676(2)	163
O1W–H2W···O3^{iii}	0.84(2)	1.92(2)	2.753(2)	174(3)
2				
N3–H3A···O3^{iv}	0.86	1.99	2.844(2)	170

[a] Symmetry codes: (i) $-x+1, -y+1, -z$; (ii) $-x+1, y+1/2, -z+1/2$; (iii) $-x+1/2, y-1/2, z$; (iv) $-x, -y+1, -z+2$.

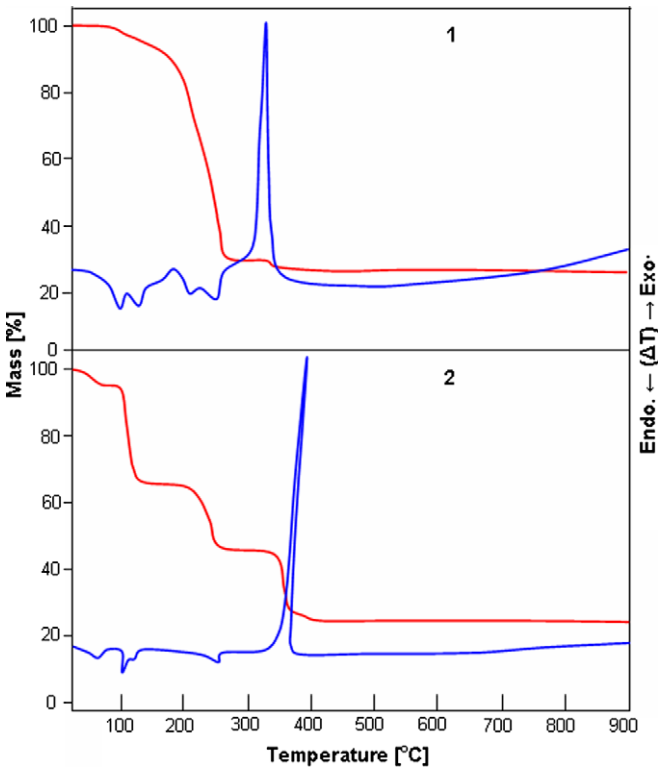

Fig. 3. DTA and TG curves of **1** and **2**.

with the calculated value of 69.9%. The decomposition ends at 349 °C, giving a final product of metallic silver.

Complex **2** displays four-stage decomposition. The presence of the lattice water molecules is evident from the TG curve (Fig. 3). The complex dehydrates in the first stage between 25 and 70 °C with a mass loss 5.3% (calcd. mass loss 6.0%). The anhydrite [Ag(barb)(dmpy)] is stable up to 98 °C and then, loses the dmpy ligand in the range 98–126 °C (the exp. mass loss 29.7%, calcd. mass loss 30.4%). The IR spectra of the residue indicates that it consist of Ag (barb) which is stable up to 193 °C. It decomposes in two stages in the temperature ranges 193–257 °C and 334–398 °C to yield an end product of the metallic silver.

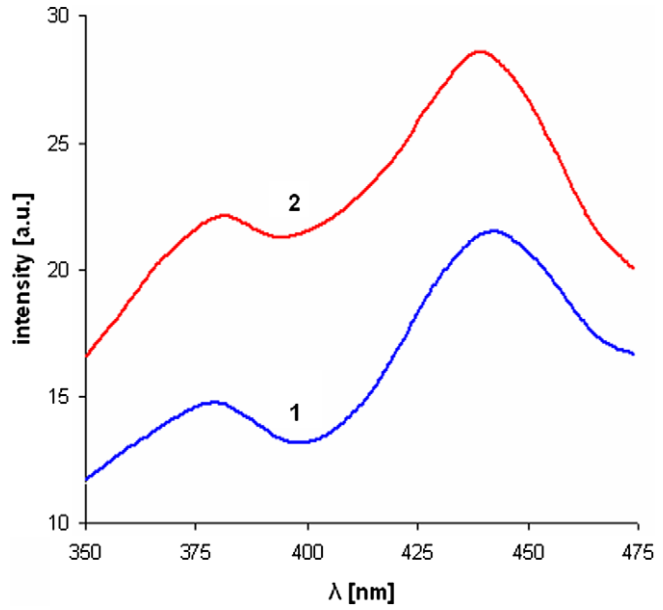

Fig. 4. The emission spectra of **1** and **2** excited at 275 nm in solid state at room temperature.

3.4. Photoluminescence

Since both ligands are liquid in room temperature, the spectra of the ligands were measured in the liquid form, while those of their complexes in the solid state at room temperature. The emission spectra of complexes **1** and **2** are shown in Fig. 4. The free pym exhibits two broad emission bands centered at 367 and 454 nm upon excitation at 272 nm. Complex **1** excited at 275 nm displays similar emission bands compared to those of pym. It emits at 382 and 443 nm. Compared to that of the free pym, a 15 nm red shift for the band centered at 367 nm and a 10 nm blue shift for the band at 454 nm were observed in the spectrum of **1**. The emission bands observed in **1** mainly arise from the aromatic pyridine chromophore in the pym ligand and tentatively assigned to π–π^* intra-ligand emissions.

The free dmpy in the liquid form displays a strong emission band at 356 nm when excited at 285 nm, while complex **2** exhibits two emission bands at 381 and 441 nm upon excitation at 275 nm, resembling the spectrum of **1** (Fig. 4). The observations show that the emission band of the ligand is significantly red-shifted upon complexation. Since intermolecular interactions such as π stacking and hydrogen bonding play an essential role in decreasing the HOMO–LUMO gaps [27–30], the remarkable red shift is probably caused intermolecular interactions involving the dmpy ligand in the solid complex of **2**. Again, the emission bands in the spectra of **2** may be originated from the π–π^* emissions of the coordinated dmpy ligand at the excited state.

4. Conclusions

Two new silver(I)-barb complexes with pym and dmpy have been synthesized and characterized. The mononuclear complexes are doubly bridged by hydrogen bonds between the barb ligands and the dimeric units are extended into a two-dimensional supramolecular structure by weak Ag···C interactions between the silver(I) ion and the py ring of the pym and dmpy ligands. Both complexes are the first examples of extended silver(I)-barb structures generated from Ag···C_{py} interactions and it appears that in the both complexes, the weak Ag···C interactions play an essential role in packing of molecules and also the structural dimensionality. Both complexes manifest luminescence properties which are modified by the present intermolecular interactions.

5. Supplementary material

CCDC 728643 and 728644 contain the supplementary crystallographic data for **1** and **2**. These data can be obtained free of charge from The Cambridge Crystallographic Data Centre via www.ccdc.cam.ac.uk/data_request/cif.

Acknowledgement

We thank the research fund of Uludag University for the financial support given to the research project (F-2008/56).

References

[1] W.J. Doran, in: F.F. Blicke, R.H. Cox (Eds.), Medicinal Chemistry IV, John Wiley, New York, 1959, p. 334.
[2] J.J.L. Zwikker, Pharm. Weekblad 68 (1931) 975.
[3] L. Levi, C.E. Hubley, Anal. Chem. 28 (1956) 1591.
[4] B.C. Wang, B.M. Craven, Chem. Commun. (1971) 290.
[5] L.R. Nassimbeni, A. Rodgers, Acta Crystallogr. B 30 (1974) 2593.

[6] M.R. Caira, G.V. Fazakerley, P.W. Linder, L.R. Nassimbeni, Acta Crystallogr. B 29 (1973) 2898.
[7] G.V. Fazakerley, P.W. Linder, L.R. Nassimbeni, A.L. Rodgers, Inorg. Chim. Acta 9 (1974) 193.
[8] L. Nassimbeni, A. Rodgers, Acta Crystallogr. B 30 (1974) 1953.
[9] F. Yilmaz, V.T. Yilmaz, C. Kazak, Z. Anorg. Allg. Chem. 631 (2005) 1536.
[10] V.T. Yilmaz, F. Yilmaz, H. Karakaya, O. Buyukgungor, W.T.A. Harrison, Polyhedron 25 (2006) 2829.
[11] F. Yilmaz, V.T. Yilmaz, E. Bicer, O. Buyukgungor, Z. Naturforsch. 61b (2006) 275.
[12] F. Yilmaz, V.T. Yilmaz, E. Bicer, O. Buyukgungor, J. Coord. Chem. 60 (2007) 777.
[13] F. Yilmaz, V.T. Yilmaz, H. Karakaya, O. Buyukgungor, Z. Naturforsch. 63b (2008) 134.
[14] V.T. Yilmaz, M.S. Aksoy, O. Sahin, Inorg. Chim. Acta 362 (2009) 3703.
[15] M.S. Aksoy, V.T. Yilmaz, O. Buyukgungor, J. Coord. Chem., in press, doi:10.1080/00958970903051924.
[16] Stoe & Cie, X-RED32 (Version 1.04), Stoe & Cie, Darmstadt, Germany, 2002.
[17] G.M. Sheldrick, Acta Crystallogr. A 64 (2008) 112.
[18] A.L. Spek, J. Appl. Crystallogr. 36 (2003) 7.
[19] R. Sneider, M.W. Hosseini, J.-M. Planeix, A.D. Cian, J. Fischer, Chem. Commun. (1998) 1625.
[20] A.J. Blake, G. Baum, N.R. Champness, S.S.M. Chung, P.A. Cooke, D. Fenske, A.N. Khlobystov, D.A. Lemenovskii, W.S. Li, M. Schroder, J. Chem. Soc., Dalton Trans. (2000) 4285.
[21] M. Mascal, J.L. Kerdelhue, A.J. Blake, P.A. Cooke, R.J. Mortimer, S.J. Teat, Eur. J. Inorg. Chem. (2000) 485.
[22] A.N. Khlobystov, A.J. Blake, N.R. Champness, D.A. Lemenovskii, A.G. Majouga, N.V. Zyk, M. Schroder, Coord. Chem. Rev. 222 (2001) 155.
[23] H.-Y. Liu, H. Wu, J.-F. Ma, S.-Y. Song, J. Yang, Y.-Y. Liu, Z.-M. Su, Inorg. Chem. 46 (2007) 7299.
[24] L. Zhao, X.-Li Zhao, T.C.W. Mak, Chem. Eur. J. 13 (2007) 5927.
[25] K. Akhbari, A. Morsali, S. Rafiei, M. Zeller, J. Organomet. Chem. 693 (2008) 257.
[26] V.T. Yilmaz, S. Hamamci, C. Kazak, J. Organomet. Chem. 693 (2008) 3885.
[27] B. Valeur, Molecular Fluorescence: Principles and Applications, Wiley-VCH, Weinheim, 2002.
[28] P. Cassoux, Science 291 (2001) 263.
[29] A. Kobayashi, H. Tanaka, H. Kobayashi, J. Mater. Chem. 11 (2001) 2078.
[30] H. Tanaka, Y. Okano, H. Kobayashi, W. Suzuki, A. Kobayashi, Science 291 (2001) 285.